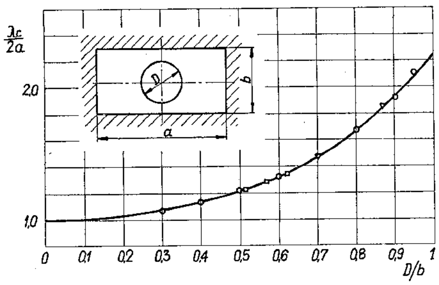

Fig. 1. TE_{11} mode cutoff wavelength. ∇, O, and □ measured in band 8 mm, 3 cm, and 4.5 cm, respectively.

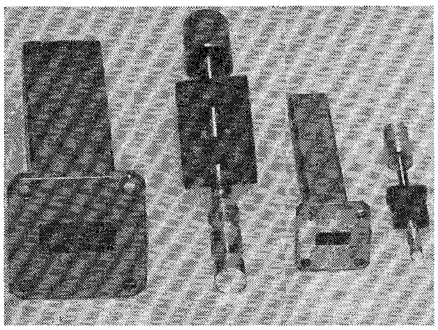

Fig. 2. Four sectional waveguide shorts.

where

λ_c = cutoff wavelength
a = waveguide width
b = waveguide height
D = rod diameter.

When $D=0$, the equation reduces to the expression for the cutoff wavelength of the TE_{10} mode in rectangular guide; the TE_{11} mode is no longer present.

The cutoff wavelength in the waveguide has been determined by wavelength measurements. Rods of various diameters have been placed within the axis of symmetry of a slotted line made of standard waveguide sections, WR-137 (IEC R70), WR-90 (IEC R100), and WR-28 (IEC R320).

Measurements were made over three frequency bands (7.5, 10, and 36 Gc/s), and results are shown and compared with the foregoing function in Fig. 1. Results are well within 2 percent off the theoretical curve. Shorts (Fig. 2) have been built according to the plot, comprising four sections to cover 8.2 to 12.4 Gc/s and 18 to 26.5 Gc/s. The input VSWR of both shorts is over 200 ($\Gamma \geq 0.99$) in their respective frequency bands.

M. Rzepecka
S. Stuchly
UNIPAN Scientific Instruments
Polish Academy of Science
Warszawa 1,
Krajowej Rady Narodowej 51/55
Poland

References

[1] E. G. Cristal, "Coupled circular cylindrical rods between parallel ground planes," *IEEE Trans. on Microwave Theory and Techniques*, vol. MTT-12, pp. 428–439, July 1964.
[2] ——, "Characteristic impedance of coaxial lines of circular inner and rectangular outer conductor," *Proc. IEEE (Correspondence)*, vol. 52, pp. 1265–1266, October 1964.
[3] D. A. Ellerbruch, "Evaluation of microwave phase measuring system," *J. Res. NBS*, vol. 69C, pp. 55–65, January–March 1965.

An Experimental X-Band Electron-Cyclotron-Resonance Plasma Accelerator

The electron-cyclotron-resonance plasma accelerator represents a new and potentially important application of microwave power. Uses in space propulsion engines and thermonuclear energy generators are currently under investigation. In this type of accelerator, the plasma is generated and accelerated to high velocities by RF power. The high-frequency nature of the electrical energy allows efficient, electrodeless coupling to the plasma. Conduction and control of the power is also relatively easy. Finally, for the space application, a combined communication and propulsion system can reduce total system weight and complexity. With new, high efficiency RF generators now coming into being [1], [2], the efficiency of the RF energy conversion process is no longer prohibitive. This type of plasma accelerator has been previously described [3], its theoretical basis has been explored [4], [5], and results with medium [4], [5] and high power [6] experiments have been reported. This correspondence describes in more detail some of the early higher powered experiments. Although the goal of these studies has been somewhat different, the experiments have much in common with the electron-cyclotron-resonance studies at Oak Ridge National Laboratories [7]–[9] and at Saclay [10], [11].

The experimental X-band accelerator is shown in Fig. 1. RF power (8350 Mc/s) from a CW klystron (VA-823J) is delivered from a circular polarizer into the left-hand end of the accelerator. It should be noted that the

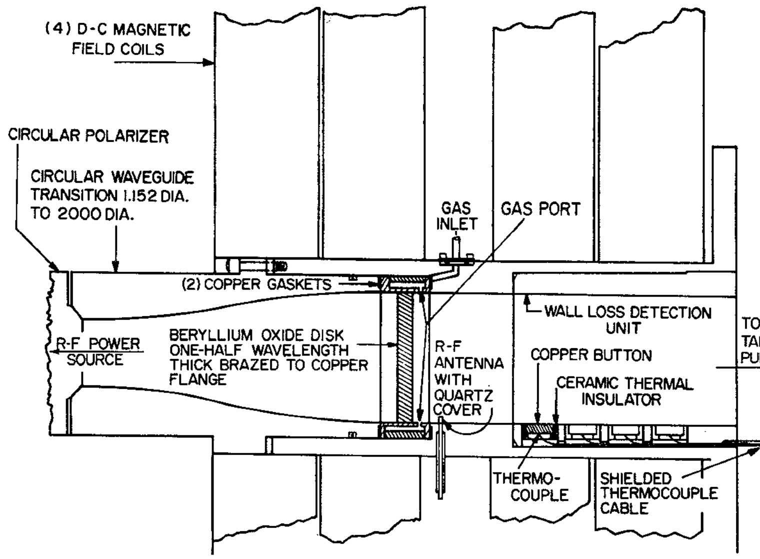

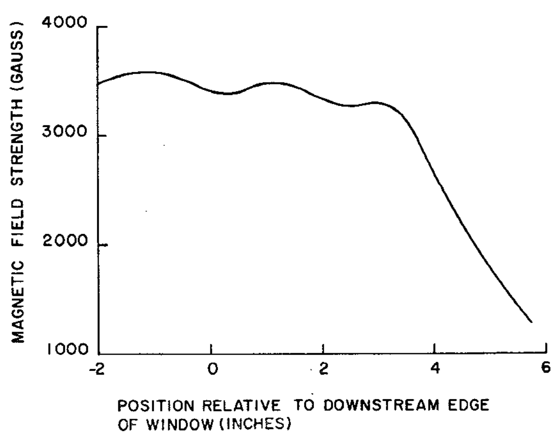

Fig. 1. X-band, longitudinal-interaction accelerator showing 3450 gauss (average) magnetic field.

Manuscript received September 22, 1965; revised November 17, 1965. This work was performed under NASA Contract NAS 3-3567.

guide cross section through the polarizer and the accelerator is circular, propagating a TE_{11} circular waveguide mode field. The RF power is then guided through a 0.286-inch thick beryllium oxide microwave window into the evacuated region. A continuous flow of gas is introduced on the vacuum side of the window. The magnetic field from the surrounding coils is adjusted approximately to the cyclotron resonance value (2970) in this region, where the injected gas is ionized and the electrons are accelerated in transverse cyclotron orbits by the microwave field. Electron trajectories are converted from transverse to longitudinal by grad B and diffusion processes, and ions are accelerated by the charge-separation field as the gas stream flows down the accelerator duct and out into the vacuum tank.

The RF frequency is measured by a precision cavity frequency meter; the frequency is held at 8350 Mc/s by adjustment of the driver klystron. RF power is determined by a matched calorimetric power meter, and power reflection coefficient is obtained using a waveguide reflectometer system. An E-H tuner between the accelerator and the reflectometer is used to minimize reflection; generally, the power reflection coefficient could be reduced to 0.1 or less. Gas flow rate is determined by measuring the time rate of change of pressure in the gas reservoir tank. Argon was used in all tests reported in this correspondence. It was found that helium resulted in a very low power efficiency. A calibrated flux meter is used to measure the magnetic field strength and shape.

The temperature of copper buttons located in the accelerator walls, as shown in Fig. 1, were determined by thermocouples. Knowing temperature change during a test, the time duration of the test, and the heat capacity of the buttons allows calculation of power density deposited along the wall. Measured wall power densities for the Fig. 1 accelerator were typically 1 W/cm^2 per kW RF power.

A cup-shaped calorimeter (10-inch diameter by 2 inches deep, with radial baffles within the cup) was mounted 28 cm beyond the accelerator exit orifice to intercept the total stream and therefore yield a measure of the total plasma stream power. Power is calculated from the steady-state difference between inlet and outlet temperatures of water used to cool the calorimeter.

This accelerator was exhausted into an 18-inch diameter vacuum tank, which was connected through a 10-inch valve to the pumping system. At the argon flow rates utilized in these experiments, the 18-inch tank pressure was approximately 1×10^{-4} torr, as measured by a cold-cathode ionization gauge.

RF antenna probes (Fig. 1) were located one centimeter and two-and-one-half centimeters beyond the vacuum edge of the window. These showed that the RF is essentially completely attenuated at the downstream probe location, indicating that the thickness of the RF plasma interaction region can be estimated to be about two centimeters.

One interesting result which was observed was the fact that, while the power reflection coefficient increases with power, the overall power conversion efficiency (plasma stream power/incident RF power) remains approximately constant, indicating that the device becomes more efficient in converting *absorbed* power to plasma stream power as the RF level increases.

Further operating characteristics are summarized subsequently. Although the data scatter is considerable, partly due to tuning having been employed in varying degrees during these tests, the following items are noted.

1) Efficiency exhibits a broad maximum as a function of flow rate, with the peak occurring at about 0.5 mg/s.

2) A magnetic field of approximately 3350 gauss (average) maximizes the efficiency. (When the tuner is left untouched and magnetic field is varied, the reflection coefficient shows a sharp drop and the propagation depth rapidly increases at approximately this same magnetic field strength.)

3) Relatively long operating times (up to 139 seconds at 3290 W RF) have been achieved at appreciable power levels. During the longer tests, engine temperatures were observed to reach an essentially steady level.

4) The maximum RF to plasma stream power conversion efficiency for this accelerator is approximately 0.25.

A three-unit sampling probe array was used to measure the exhaust stream power profile. In each of these probes, the plasma passes through a gridded orifice and deposits its energy in a collector cup. The plasma power density is then obtained from the measured heating rate of the collector and the known orifice area. The stream is found to peak approximately on axis. Furthermore, these curves reveal that the rate of stream divergence is significantly less than the magnetic field, indicating that the plasma particles are not tightly bound to magnetic field lines.

The side wall area of the accelerator is about 200 cm^2. We note, therefore, from the wall calorimeter results reported above, that something on the order of a quarter of the

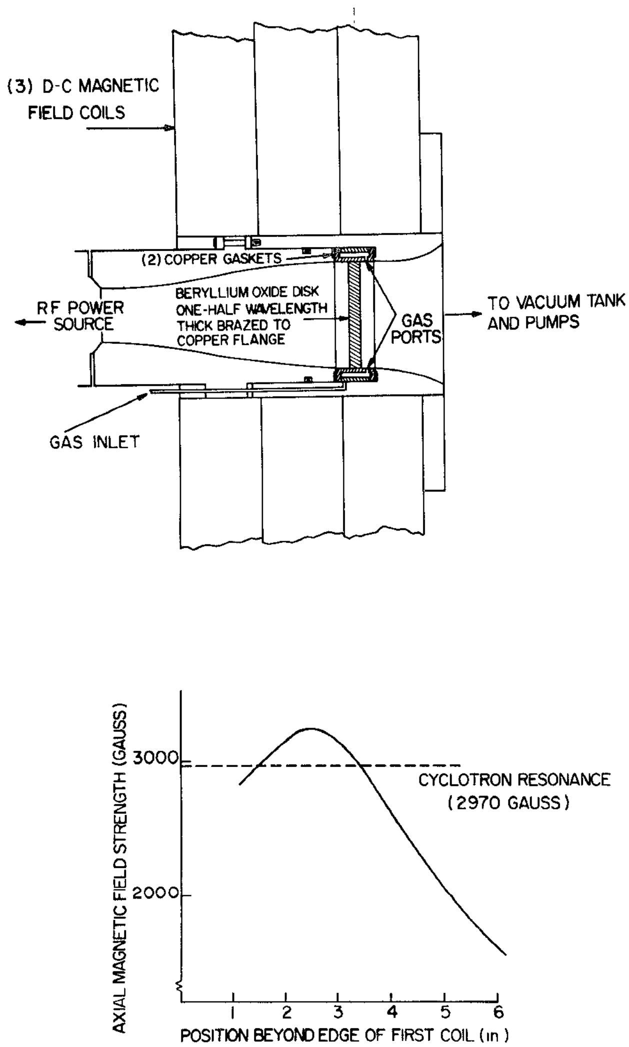

Fig. 2. Longitudinal interaction accelerator, short version.

RF power is being lost to the accelerator walls. In addition, the RF antenna probes indicate that the microwave field penetrates only a short distance beyond the dielectric window. The shorter accelerator shown in Fig. 2 was therefore built in hopes of recovering the power lost to the walls of the longer device without changing the RF/plasma interaction situation.

A dramatic increase in power received by the 10-inch diameter calorimeter was in fact observed. Typifying the operation of this shorter accelerator is a test run at 2600 watts incident RF power. The argon flow rate was 1.0 mg/s, and the magnetic field strength at the window was at the cyclotron resonance point, 2980 gauss. Tuning resulted in a power reflection coefficient of 0.02. This test lasted 203 seconds. The calorimetrically measured plasma stream power throughout this test was 1400 ± 70 watts, giving a power conversion efficiency of 0.54 ± 0.03. Although in repeated tests under different field, power and flow conditions failed to reach this high a value, all measured efficiencies were over 0.4.

For the conditions of the test described above, the mass flow rate, 1 mg/s, corresponds to a particle rate of 1.5×10^{19} argon gas molecules per second. The plasma stream carried 1400 watts to the calorimeter, or 580 eV per molecule. If this power is indeed totally transferred to directed motion of the argon ions, the average ion velocity would be 5.3×10^4 meters per second. The stream density would be 5.6×10^{10} particles per cm^3, assuming a 25-cm stream diameter.

The most obvious reason for attaining this significant result is the shortening of the plasma chamber, thereby presumably recovering a good portion of the power which, in the longer accelerator, had been measured to be going into the plasma chamber walls. It is probable that the increase in the field gradient adjacent to the window was also beneficial. A third, possibly influential change from the earlier design is the contouring of the exit orifice (compare Figs. 1 and 2).

Acknowledgment

The author wishes to acknowledge the contributions made to this program by Drs. F. W. Mezger and P. Gloersen of the General Electric Space Sciences Laboratory, King of Prussia, Pa., and Dr. H. G. Kosmahl of the NASA-Lewis Research Center, Cleveland, Ohio. In addition, C. N. Brooks should be noted for his aid in design, construction, and operation of the experimental apparatus.

David B. Miller
Space Sciences Lab.
General Electric Co.
King of Prussia, Pa.

References

[1] L. E. Brown, "Crossed-field forward wave amplifiers offer new advantages for radar systems," *Microwave J.*, vol. 7, no. 5, p. 66, May 1964.
[2 D. H. Priest and W. J. Leidigh, "A two-cavity extended interaction klystron yielding 65 per cent efficiency," *IEEE Trans. on Electron Devices*, vol. ED-11, pp. 369–373, August 1964.
[3] D. B. Miller, P. Gloersen, E. F. Gibbons, and D. J. Ben Daniel, *Engineering Aspects of Magnetohydrodynamics*, Proc. 3rd Symp., University of Rochester, N. Y., March 1962. New York: Gordon & Breach Science Publ., 1964, p. 405.
[4] H. W. Hendel and T. T. Reboul, *American Institute of Aeronautics and Astronautics J. Preprint*, no. 63001, March 1963.
[5] David B. Miller and Edward F. Gibbons, "Experiments with an electron cyclotron resonance plasma accelerator," *American Institute of Aeronautics and Astronautics J.*, vol. 2, p. 36, January 1964.
[6] David B. Miller, *AIAA Bull.*, vol. 1, p. 389, 1964.
[7] R. J. Kerr, R. A. Dandl, H. O. Eason, A. C. England, M. C. Becker, and W. B. Ard, *Bull. Amer. Phys. Soc.*, vol. 7, p. 290, 1962.
[8] W. B. Ard, M. C. Becker, R. A. Dandl, H. O. Eason, A. C. England, and R. J. Kerr, *Phys. Rev. Lett.*, vol. 10, p. 87, 1963.
[9] R. A. Dandl, "Preliminary results from a 50-liter electron-cyclotron plasma," *Bull. Amer. Phys. Soc.*, vol. 9, p. 332, March 1964.
[10] T. Consoli and R. Hall, *CR Acad. Sci. (France)*, vol. 257, p. 2804, November 4, 1963.
[11] R. Bardet, T. Consoli, and R. Geller, "Acceleration continue de plasma à gradients de champs electromagnetique et magnetique statique. Resultats experimentaux," *Phys. Letters*, vol. 10, p. 67, May 1964.

Corrections

Organic Superconductor and Dielectric Infrared Waveguide, Resonator, and Antenna Models of Insects' Sensory Organs[1]

1) Reference [6] in the text (page 707) should read [8].

2) "Metallic films [11]" in the text (page 707, 13th line of second paragraph from the end of the article) should read "metal-like films [11]." While this also allows consideration of multiple film interference with interposed absorption, according to Heavens[2] and Vasicek,[3] it does not eliminate "metal"-dielectric films.[2,4]

E. C. Okress
Amer. Stand. Research Labs.
New Brunswick, N. J.

Manuscript received November 1, 1965; revised November 15, 1965.

[1] E. C. Okress, *IEEE Trans. on Microwave Theory and Techniques (Correspondence)*, vol. MTT-13, pp. 706–707, September 1965.
[2] O. S. Heavens, *Optical Properties of Thin Solid Films*. New York: Academic, 1955.
[3] A. Vasicek, *Optics of Thin Films*. New York: Inter-Science Pub., 1960.
[4] M. Born and E. Wolf, *Principles of Optics*. New York: Pergamon, 1959, sect. 7.6.6.

Microwave Band-Stop Filters with Narrow Stop Bands[1]

Equation (17) on page 419 should have read:

$$G(\phi) = 2F(\phi) + \frac{2\delta - \sin 2\delta}{1 - \cos 2\delta}.$$

The approximation

$$G(\phi) \approx 2F(\phi)$$

still holds for ϕ close to 90 degrees. The formula has been referred to in other works.[2,3]

Leo Young
Head, Microwave Techniques Program
Electromagnetic Techniques Laboratory
Stanford Research Institute
Menlo Park, Calif.

Manuscript received January 19, 1966.

[1] L. Young, G. L. Matthaei, and E. M. T. Jones, *IEEE Trans. on Microwave Theory and Techniques*, vol. MTT-10, pp. 416–427, November 1962.
[2] J. J. Taub and R. L. Sleven, "Design of band-stop filters in the presence of dissipation," *IEEE Trans. on Microwave Theory and Techniques*, vol. MTT-13, pp. 589–616, September 1965.
[3] G. L. Matthaei, L. Young, and E. M. T. Jones, *Microwave Filters, Impedance-Matching Networks and Coupling Structures*. New York: McGraw-Hill, 1964, p. 739.

Acceptable Mode Types for Inhomogeneous Media[1]

Maxwell's equations, (1) and (2), should have been $\nabla \times \overline{E} = -j\omega\mu\overline{H}$ and $\nabla \times \overline{H} = j\omega\epsilon\overline{E}$.

The last term in (9) is a vector, i.e., $-\nabla^2\overline{H}$.

The letter H was omitted from (18); it should have read

$$\frac{\partial}{\partial x} H_y \frac{\partial}{\partial y} \ln (\mu\epsilon) = 0.$$

Four lines further—first appearances notwithstanding—the second case listed should have been described as a *particular* one and not as a *peculiar* one.

In the center column of page 876, the last sentence of the first paragraph should be amended to " . . . the normal modes must still be of the LS type . . . "

In reference [8], a transposition occurred in the spelling of the name of G. Barzilai.

A. Wexler
Dept. of Elec. Engrg.
Imperial College
London, England

Manuscript received January 31, 1966.

[1] A. Wexler, *IEEE Trans. on Microwave Theory and Techniques*, vol. MTT-13, pp. 875–878, November 1965.